Adsorption and Reaction of Nitric Oxide with Atomic Oxygen Covered Au(111)

Sean M. McClure, Tae S. Kim, James D. Stiehl, Paul L. Tanaka, and C. Buddie Mullins*

Department of Chemical Engineering, University of Texas at Austin, 1 University Station, C0400 Austin, Texas 78712-0321

Received: June 18, 2004; In Final Form: September 9, 2004

Molecular beam scattering techniques were employed to investigate the adsorption/reaction of NO with an atomic oxygen covered Au(111) surface to form nitrogen dioxide, NO_2. Results suggest that at temperatures above $T_s \approx 200$ K, the NO_2 production is limited by NO surface lifetime on O/Au(111); at temperatures below $T_s \approx 200$ K NO_2 production is limited by both a reduction in the NO_2 reaction rate and NO_2 desorption limitations. Collision induced desorption (CID) and temperature programmed desorption (TPD) spectra provide evidence that suggests nitric oxide may react with chemisorbed oxygen atoms at temperatures as low as $T_s \approx 85$ K. A simple kinetic model was employed to estimate the activation energy ($E_r \approx 0.21 \pm 0.02$ eV) of this reaction on the Au(111) surface with an atomic oxygen coverage of $\theta_o \approx 0.95$ ML. These results illustrate that while bulk gold surfaces are generally considered to be catalytically inert, the presence of chemisorbed atomic oxygen significantly increases the adsorption/reactive properties of the Au(111) surface toward gas-phase nitric oxide.

Introduction

Though traditionally regarded as the most noble of the transition metals,[1,2] lately gold has received much attention as an attractive material for heterogeneous catalysis, particularly when present as Au nanoclusters supported on metal oxide (TiO_2, Al_2O_3) surfaces.[3−10] The recent discovery of the catalytic activity of metal oxide supported Au clusters has spurred a renewed interest in investigating the chemistry of bulk gold surfaces. Insights gleaned from studies of bulk gold surface reactions will assist in a deeper understanding of the chemistry occurring on metal oxide supported Au nanoparticles. While bulk gold does not easily adsorb or dissociate molecular oxygen[11−13] it does readily chemisorb oxygen in its *atomic* form when the Au surface is exposed to O_3, atomic oxygen sources, or when physisorbed oxygen is dissociated on the surface at low temperature via electron bombardment.[14,15] When atomic oxygen is present on bulk gold surfaces, it has been shown to be quite reactive with a variety of molecules such as CH_3OH, CO, C_2H_4, and formaldehyde.[16−19]

It has been illustrated experimentally that nitrogen oxides, such as NO, NO_2, and N_2O_3, exhibit interesting chemistry on bulk gold surfaces. Work by Bollinger et al. has shown that the reduction of nitrogen dioxide and nitric acid with carbon monoxide over a heated gold surface can be used to measure the concentration of nitrogenous species in the atmosphere.[20] A number of investigations have revealed gold (both bulk gold and gold nanoclusters) to have applications as sensors for gas-phase NO and NO_2 species.[21−23] A number of insightful studies by Koel et al.[14,19,24−25] have shown that nitrogen oxides (NO_2, NO, N_2O_3) exhibit a rich chemistry on gold surfaces and, in particular, oxygen covered gold surfaces.

Few studies to date have been conducted investigating the interaction of NO with Au and oxygen covered Au surfaces.[26,27]Ardebili et al. performed an ultrahigh vacuum (UHV) study of the chemiluminescence resulting from the reaction of nitric oxide and atomic oxygen on a polycrystalline Au sample, which was preexposed to atomic oxygen at temperatures as low as $T_s \approx 195$ K.[26] NO and oxygen atoms were simultaneously dosed onto the polycrystalline sample and it was shown that the reaction chemiluminescence was dependent on the preexposure of the polycrystalline Au surface to atomic oxygen. Here, we report on the results of our molecular beam investigation of the adsorption and reaction of NO with an atomic oxygen covered Au(111) surface under UHV conditions, and how this adsorption/reaction is affected by surface temperature and oxygen adatom coverage.

Experimental Section

Experiments for this study were conducted in an ultrahigh vacuum (UHV)/molecular beam chamber described in detail in previous publications (base pressure $< 2 \times 10^{-10}$ Torr).[5,18,28−29] Experiments were performed on a sample assembly that consists of an Au(111) single crystal (∼1 cm diameter) and an Au/TiO_2 model catalyst sample (used in other studies[18,29]) mounted on opposing sides of a tantalum plate. The sample is resistively heated and cooled via thermal contact with a liquid nitrogen reservoir (sample assembly cools rapidly to $T_s \approx 85$ K; mechanical pumping on the liquid nitrogen reservoir provides rapid cooling to $T_s \approx 77$ K). Au(111) surface cleanliness and order were verified via Auger electron spectroscopy (AES) and low-energy electron diffraction (LEED). A radio frequency (RF) generated plasma jet source was used to populate the Au(111) surface with oxygen atoms (O^{16} and O^{18}).[30−32] An 8% O_2/92% Ar gas mixture was employed to create the O-atom plasma, with ∼40% of the oxygen molecules dissociated, as determined via time-of-flight techniques (TOF).[31,32] Reported atomic oxygen coverages, θ_o, are absolute oxygen coverages estimated by comparing the O(510 eV)/Au(238 eV) Auger peak ratios[18] for a given oxygen dose with the literature value of O(510 eV)/Pt(237 eV) ≈ 0.3 for a Pt(111) surface saturated with atomic oxygen (correcting for Au and Pt Auger sensitivities).[33] At

* To whom correspondence should be addressed. E-mail: mullins@che.utexas.edu.

10.1021/jp047335d CCC: $27.50
Published on Web 10/26/2004

saturation, atomic oxygen forms a (2 × 2) ordered overlayer on the Pt(111) surface, thus allowing an estimate of the absolute oxygen coverage on the Au(111) surface.[34] A room temperature, pure NO molecular beam (typical flux ≈ 1×10^{13} molecules cm^{-2} s^{-1}) was used to deliver nitric oxide to the Au(111) surface. A high kinetic energy (~1 eV) Kr beam (a 2% Kr in He gas mixture) was used for collision induced desorption (CID) experiments.[29,35] A room temperature, pure nitrogen dioxide (NO_2) beam was used to deliver NO_2 to the Au(111) surface. NO_2 flux and coverage values were determined by the dose time required to populate the chemisorbed NO_2 monolayer on Au(111).[24] The NO, NO_2, and Kr/He beams were all dosed through the RF nozzle with the RF power source disabled. Hence, the impingement area (~7 mm^2) of the O, NO, NO_2, and 2% Kr/He beams are the same and are smaller than the area of the Au(111) single-crystal sample to minimize direct exposure of other surfaces in the UHV chamber. An inert flag is located in the UHV scattering chamber that can be moved in and out of the beam path to perform King and Wells reflectivity measurements.[36] King and Wells reflectivity experiments measure the *reflected* beam signal, i.e., the molecules in the beam which are reflected from the sample surface. When this reflected QMS signal from the sample is compared to the QMS signal of the beam impinging on the inert flag, relative gas uptake measurements can be obtained. Initial adsorption probabilities, S_o, of nitric oxide were obtained in a similar fashion. First, a nitric oxide beam is allowed to strike the sample and the reflected NO signal (I_{sample}) is measured *immediately* after the NO beam impinges upon the sample. Then, in a separate measurement, the NO beam is directed onto the inert flag and the reflected NO signal from when the beam *first* strikes the inert flag (I_{flag}) is measured. The initial adsorption probability, S_o, can then be estimated from the ratio of these signals: $S_o = (1 - I_{sample}/I_{flag})$.

Finally, in a previous study[29] we have shown that our RF oxygen plasma generates a small amount of adsorbed molecular oxygen on the Au(111) sample at temperatures below $T_s \approx 150$ K. Hence, after each atomic oxygen dose, the sample is annealed to $T_s \approx 300$ K, a temperature sufficiently below the atomic oxygen recombinative desorption temperature of $T_s \approx 540$ K, to remove any molecular oxygen species populating the Au(111) surface. Therefore, the impinging NO molecule is interacting with a Au(111) surface populated entirely by chemisorbed *atomic* oxygen species.

Results and Discussion

Adsorption of NO on Au(111). Shown in Figure 1 are NO temperature programmed desorption (TPD) spectra and collision induced desorption (CID) spectra from the clean Au(111) surface after exposure to a pure NO beam at $T_s \approx 77$ K. A peak desorption temperature of $T_s \approx 150$ K is observed in Figure 1a, which corresponds to an adsorption energy of approximately ~0.4 eV, assuming first-order desorption kinetics (with a preexponential factor of $\upsilon_d \approx 10^{13}$ s^{-1}).[37] The presence of surface nitric oxide is further verified by the CID spectra shown in Figure 1c. Curve c shows collision induced desorption of nitric oxide from the Au(111) surface at $T_s \approx 77$ K. Curves d and e are collision induced desorption spectra obtained following dosing of nitric oxide on an *inert flag* and following dosing of nitric oxide on the Au(111) surface and heating to $T_s \approx 300$ K, respectively. Curve b shows a TPD spectra obtained after NO is dosed to the Au(111) surface at $T_s \approx 77$ K and swept prior to TPD heating. The absence of any nitric oxide evolution from the Au(111) surface in curves b and e provides evidence that

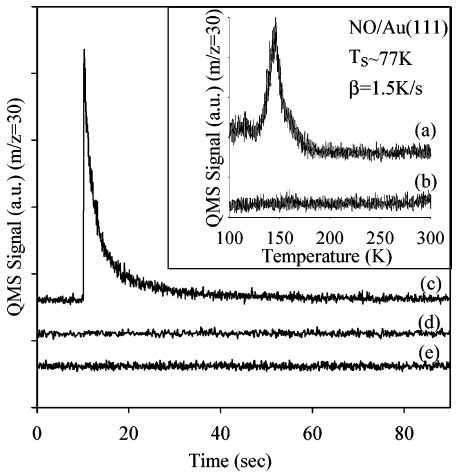

Figure 1. NO TPD spectra from Au(111) following (a) 5 s NO exposure at 77K, (b) 5 s NO exposure at $T_s \approx 77$ K and Kr sweep, and collision induced desorption (CID) spectra obtained at $T_s \approx 77$ K following (c) 5 s NO exposure at 77 K, (d) 5 s NO exposure *on inert flag*, (e) 5 s NO exposure at $T_s \approx 77$ K followed by heating to $T_s \approx 300$ K. In CID spectra, the Kr beam impinges on the sample at $t = 10$ s. NO beam flux (F): 1×10^{13} molecules cm^{-2} s^{-1}.

nitric oxide is adsorbed on the Au(111) sample and is removed after heating above $T_s \approx 175$ K. This finding is in contrast with that obtained by Koel and co-workers, who observed no nitric oxide adsorption on Au(111) down to temperatures of $T_s \approx 95$ K, obtained by directed dosing of a Au(111) sample under UHV conditions.[24] We speculate that this discrepancy is probably attributable to differences in the concentration of surface defects and steps present on the different Au(111) crystal samples. To our knowledge, no other experimental studies of NO adsorption have been conducted on more corrugated Au single crystal surfaces. However, recent DFT calculations of NO adsorption on tetrahedral Au clusters have shown that NO adsorption on Au clusters is thermodynamically favorable ($E_{ads} = 1.34$ eV), with the nitric oxide molecule bonding to Au via its nitrogen atom.[38] These results support the idea that NO may be able to adsorb to uncoordinated Au atoms, such as those at surface defect sites and steps or on Au nanoparticles. Indeed, spectroscopic evidence for NO adsorption on metal oxide supported Au catalysts has been observed. High-pressure (0.3−10 bar) FTIR studies of NO on Au/TiO_2 by Debeila et al.[39] and Solymosi et al.[40] gave vibrational frequencies that they attributed to the presence of molecularly adsorbed NO and $(NO)_2$ species on gold cluster sites. King and Wells reflectivity measurements[36] (not shown) indicate negligible adsorption of NO on clean Au(111) at surface temperatures above $T_s \approx 150$ K. This result is in agreement with the findings of Koel and co-workers for temperatures *above* $T_s \approx 150$ K, for NO/Au(111).[24] There is no evidence of NO dissociation on either the clean or oxygen covered Au(111) surface at any of the temperatures studied ($T_s \approx 77$ to 700 K) under UHV conditions, as determined by the absence of O_2, N_2, or NO recombinative desorption TPD after nitric oxide exposure.

Adsorption of NO on O/Au(111). Shown in Figure 2 are NO uptake measurements as a function of oxygen adatom coverage at $T_s \approx 85$ K. While a small amount of NO is adsorbed on the clean Au(111) surface (likely at defects and steps) at $T_s \approx 85$ K, much more nitric oxide is taken up by oxygen covered Au(111). As oxygen atoms are introduced to the Au(111) surface, both the initial and the absolute NO uptake begin to increase with increasing atomic oxygen coverage. As the oxygen coverage reaches a value of $\theta_o \approx 0.32$ ML and increases to $\theta_o \approx 0.89$ ML, the absolute uptake of nitric oxide begins to

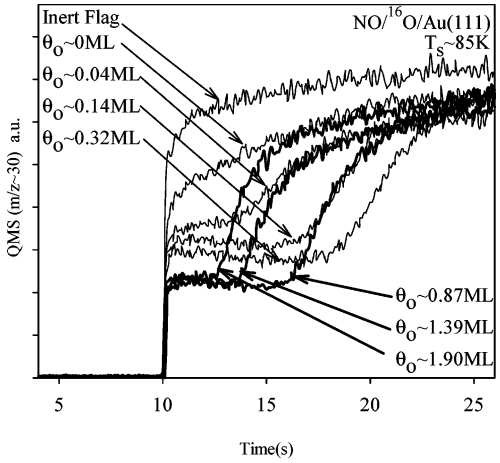

Figure 2. Nitric oxide uptake measurements obtained for various atomic oxygen coverages; $\theta_o \approx 0$, 0.04, 0.32, 0.87, 1.4, 1.9 ML, and on inert flag at $T_s \approx 85$ K. At $t = 10$ s, the NO beam impinges on the ^{16}O atom covered Au(111). NO beam flux (F): 1×10^{13} molecules cm^{-2} s^{-1}.

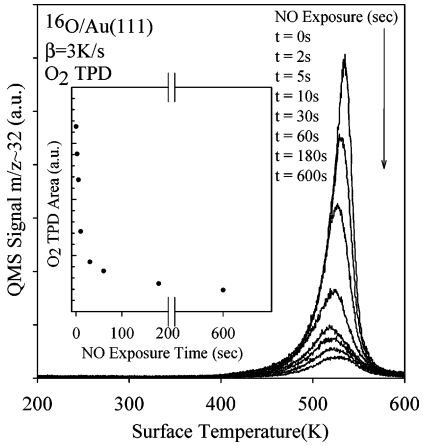

Figure 3. O_2 TPD spectra obtained after exposing an oxygen covered ($\theta_o \approx 0.95$ ML) Au(111) surface to varying amounts of NO at $T_s \approx 85$ K and subsequent heating. Curves correspond to exposures of $t = 0$, 2, 5, 10, 30, 60, 180, and 600 s of NO exposure, respectively. NO beam flux (F): $\sim 1 \times 10^{13}$ molecules cm^{-2} s^{-1}.

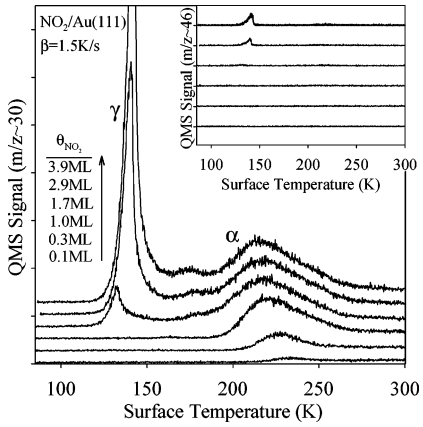

Figure 4. NO_2 TPD spectra from Au(111) surface. NO_2 is impinged on the Au(111) sample at 85 K for various NO_2 exposures. The sample is then heated at a TPD ramp rate of $\beta = 1.5$ deg/s. NO_2 beam flux: ~0.4 ML/s.

decrease as the oxygen adatom coverage is increased, with the initial NO uptake remaining relatively constant, $S_o \approx 0.7$.

From this series of NO uptake measurements it appears that the presence of chemisorbed oxygen atoms enhances the ability of the Au(111) surface to uptake nitric oxide. Interestingly, it appears that only a relatively small amount of atomic oxygen ($\theta_o \approx 0.04$ ML) is necessary to bring about increased NO adsorption on the gold surface. Indeed, previous investigations of the atomic oxygen on bulk gold have illustrated that chemisorbed oxygen atoms can alter the electronic properties of Au surfaces. Measurements conducted by Saliba et al.[14] indicate that the presence of oxygen atoms on the gold surface increases the work function of the Au surface by 0.81 eV at an oxygen atom coverage of $\theta_o \approx 1.0$ ML. Similar oxygen induced work function changes have also been observed on the Au(110)−(1 × 2) surface.[41] The effect of low coverages of adsorbates on the electronic structure of metal surfaces has been studied both computationally and experimentally, and it has been shown that small amounts of adsorbates can significantly alter the electronic characteristics of the surface atoms and the binding strength of coadsorbates.[42,43] We speculate that the decrease in absolute uptake observed with increasing oxygen adatom coverage (above coverages of $\theta_o \approx 0.89$ ML) could be due to either blocking of NO adsorption sites and/or other changes (electronic, structural) in the Au surface due to the presence of additional oxygen adatoms. It is also interesting to note that with a saturation coverage of atomic oxygen ($\theta_o \approx 1.9$ ML and higher), more NO is adsorbed on the oxygen covered Au(111) than on the clean Au(111) surface. Additional King and Wells reflectivity measurements of the adsorption of NO on an O/Au(111) surface with $\theta_o \approx 0.95$ ML show negligible adsorption of NO at temperatures above $T_s \approx 300$ K. These data suggest that at these elevated temperatures ($T_s > 300$ K), the surface lifetime of the adsorbed NO molecule on the *oxygen-covered Au(111) surface* is quite short relative to the experimental time scale.

Reaction of NO with ^{16}O/Au(111) and ^{18}O/Au(111). When an atomic oxygen covered Au(111) surface is exposed to a NO molecular beam, oxygen adatoms are depleted, as observed in the loss of signal in the O_2 recombinative TPD spectra. Figure 3 shows recombinative oxygen desorption spectra after various NO doses on an oxygen covered Au(111) surface, with an initial oxygen coverage of $\theta_o \approx 0.95$ ML at 77 K. A similar reduction in the O_2 TPD spectra area is also observed when NO is dosed on oxygen covered surfaces at higher temperatures ($T_s = 77-400$ K). However, at higher temperatures ($T_s > 77$ K) and higher coverages ($\theta_o > 0.95$ ML) the amount of oxygen removed from the surface for a given NO exposure is *decreased*. The spectra in Figure 3 illustrate that as more NO is impinged on the O/Au(111) surface, additional oxygen adatoms are removed upon heating. Masses corresponding to NO_2, N_2O, N_2, O_2, and N_2O_3 were monitored during reaction experiments, yet none were detected at any of the temperatures from $T_s = 77-400$ K. However, due to the difficulty in detecting NO_2 as an intact molecule ($N^{16}O^{16}O$; $m/z \sim 46$) under UHV conditions, $N^{16}O^+$ ($m/z \sim 30$) is the primary fragment that would be detected in the QMS from production of an NO_2 reaction product. This was verified by adsorbing NO_2 and then performing NO_2 desorption experiments (Figure 4) from our Au(111) sample. While a small NO_2 signal ($m/z \sim 46$) (see inset of Figure 4) is seen for the desorption of large multilayer doses (γ feature), only a $m/z \sim 30$ signal, corresponding to the $N^{16}O^+$ ($m/z \sim 30$) fragment, is seen at the chemisorbed, monolayer NO_2 feature at $T_s \approx 225$ K (α feature). These desorption features are in good agreement with the NO_2 desorption features observed by Bartram et al. from Au(111) pre-dosed with NO_2.[24] To assist in the measurement of the reaction product, isotopically labeled oxygen ($^{18}O_2$) was employed. This permits detection of NO_2 ($N^{16}O^{18}O$) production from an ^{18}O covered Au(111) surface,

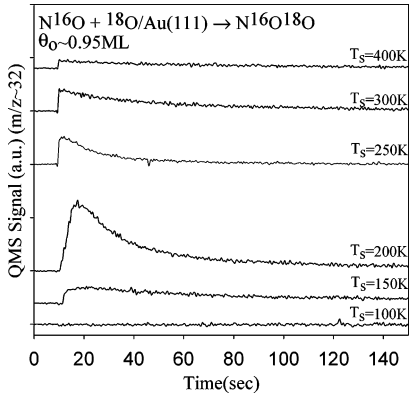

Figure 5. $N^{16}O$ impinged on ^{18}O/Au(111) surface ($\theta_o \approx 0.95$ ML) at various surface temperatures. The Au(111) sample is exposed to ^{18}O atoms at $T_s \approx 77$ K to produce an atomic oxygen coverage of $\theta_o \approx 0.95$ ML. The sample is then heated to the desired surface temperature, T_s, and the NO beam impinges on the ^{18}O/Au(111) sample at $t = 10$ s. NO beam flux (F): $\sim 9 \times 10^{13}$ molecules cm^{-2} s^{-1}. Note: The data shown have been background corrected for a relatively small amount of accumulation/production of $N^{18}O$ that occurs in the chamber, as verified by blank experiments off of the inert flag.

allowing for some differentiation between nitric oxide reactant fragments ($N^{16}O^+$) from the impinging NO beam and ($N^{18}O^+$) fragments resulting from NO_2 formation on the O/Au(111) surface. Shown in Figure 5 are $N^{18}O$ production spectra, and hence NO_2 production spectra, obtained by dosing $N^{16}O$ (via molecular beam) on an ^{18}O covered Au(111) surface ($\theta_o \approx 0.95$ ML) at various surface temperatures. As the spectra in Figure 5 illustrate, the initial NO_2 production ($N^{18}O^+$ signal) peaks at a surface temperature of $T_s \approx 200$ K and decreases as the surface temperature increases. At temperatures of $T_s \approx 200$ K and above, it appears that NO_2 is produced and promptly desorbed from the Au(111). We postulate that this decrease in the initial production rate is due to a decrease in the surface lifetime of the adsorbed NO reactant molecules at higher temperatures. At temperatures below $T_s \approx 200$ K, the initial NO_2 production ($N^{18}O^+$ signal) decreases as the temperature is decreased. We speculate that this is due to a combination of a decrease in the surface reaction rate at lower temperatures and/or a decrease in the apparent reaction rate due to NO_2 desorption limitations. Note that $N^{18}O^+$ production is seen evolving from the surface at a temperature of $T_s \approx 150$ K, approximately 45 K lower than that observed by Ardebili et al.[26]

Figure 6 shows NO_2 (detected as $N^{16}O^+$) temperature programmed reaction (TPR) spectra obtained after dosing an ($\theta_o \approx 0.95$ ML) oxygen covered sample with NO at $T_s \approx 85$ K. As the coadsorbed species (NO, O) are heated, the TPR spectra show a small $N^{16}O^+$ signal that occurs at $T_s \approx 225$ K, coincident with the NO_2 desorption peak temperature observed from our Au(111) sample (Figure 6A). When ^{18}O atoms are present on the Au(111) surface (Figure 6B), the NO_2 desorption feature splits into two components: (i) an $m/z \sim 30$ feature, which corresponds to an $N^{16}O^+$ fragment, and (ii) an $m/z \sim 32$ feature, which corresponds to the $N^{18}O^+$ fragment of the desorbing NO_2 product. From these results it appears that during TPD heating, the reaction of NO and O occurs at some intermediate reaction temperature between $T_s \approx 85$ (NO dosing temperature) and 225 K (NO_2 desorption temperature) to form a surface bound NO_2 product. Dosing the oxygen covered Au(111) sample with increasing amounts of NO at $T_s \approx 85$ K, such as those experiments shown in Figure 3, results in an *increase* in the chemisorbed NO_2 TPD feature at $T_s \approx 225$ K upon subsequent TPD.

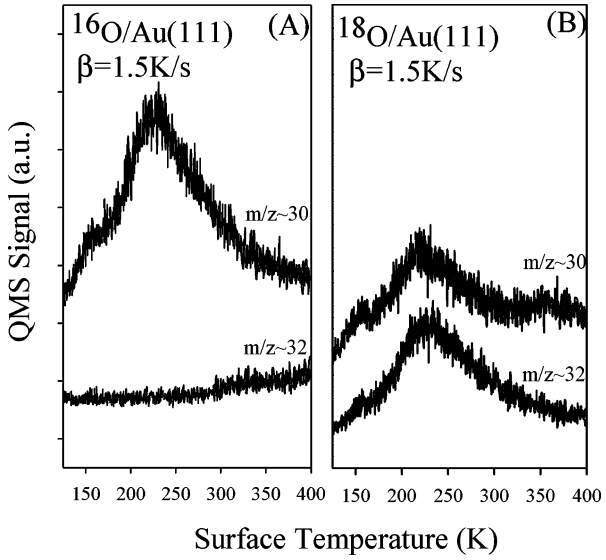

Figure 6. NO_2 TPR ($m/z \sim N^{16}O^+$; $m/z \sim N^{18}O^+$) after (A) exposure of ^{16}O covered ($\theta_o \approx 0.95$ ML) Au(111) surface and (B) exposure of ^{18}O covered ($\theta_o \approx 0.95$ ML) Au(111) surface to 30 s of NO at $T_s \approx 85$ K. NO beam flux (F): $\sim 1 \times 10^{13}$ molecules cm^{-2} s^{-1}.

No measurable NO_2 dissociation was observed on either the clean or oxygen covered (^{18}O) Au(111) surfaces under UHV conditions. This was verified by the lack of a recombinative O_2 TPD feature after the dosing of a clean Au(111) surface with NO_2 and a lack of isotopic mixing in both the NO_2 desorption feature and recombinative O_2 feature after dosing NO_2 on an ^{18}O covered Au(111) surface. The clean Au(111) result is in agreement with Bartram et al., who previously showed that NO_2 does not measurably dissociate on Au(111) under UHV conditions.[24] Additional experiments performed by the Koel group have shown that when NO_2 is dosed *on* an oxygen (^{16}O) covered Au(111) surface, a second NO_2 desorption feature begins to appear at $T_s \approx 175$ K, along with the normal NO_2 desorption feature at $T_s \approx 225$ K.[19] As the atomic oxygen coverage is increased the normal NO_2 desorption feature ($T_s \approx 225$ K) decreases, while the second NO_2 desorption feature *(*$T_s \approx 175$ K) grows, resulting in complete suppression of the normal TPD feature at oxygen coverages greater than $\theta_o \approx 1.0$ ML. Koel and co-workers speculate that this feature may be due to the formation of a nitrate species ($NO_{3,ads}$) on the Au(111) surface, but due to inherent experimental difficulties they were unable to verify this spectroscopically via HREELS measurements. We observe similar behavior in our results of NO_2 desorption from ^{18}O/Au(111) and ^{16}O/Au(111). As mentioned previously, no isotopic mixing ($N^{18}O^+$) is observed during the desorption of either of the NO_2 TPD features from the ^{18}O/Au(111) surface. This result is interesting as TPR measurements, such as those shown in Figure 6, show that the NO_2 product formed from the dosing of NO on ^{16}O/Au(111) and ^{18}O/Au(111) desorbs as it would from the clean Au(111) surface ($T_s \approx 225$ K) and with isotopic mixing from the ^{18}O/Au(111) surface. While we are only able to speculate on these results, it may be possible that NO_2, when dosed *onto* an O/Au(111) surface, can adsorb (and desorb) to regions of clean Au(111) ($T_s \approx 225$ K) and highly oxidized regions of the Au(111) surface ($T_s \approx 175$ K) with different binding strengths. As more of the surface is covered with oxygen adatoms and becomes increasingly oxidized, a larger percentage of NO_2 adsorbs and desorbs at $T_s \approx 175$ K. NO_2 formed as a reaction product of adsorbed NO and oxygen atoms on the Au(111) surface desorbs as NO_2 would from the clean Au(111) surface. This may indicate that

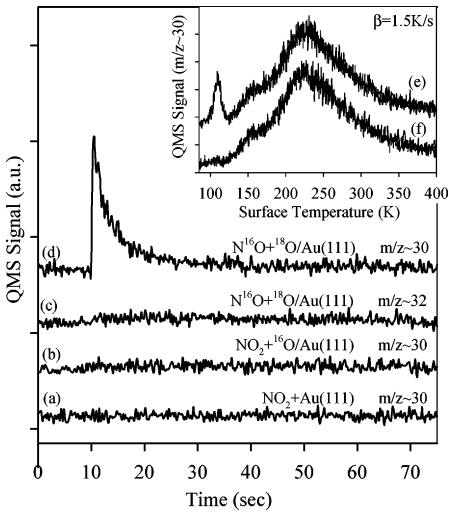

Figure 7. Kr CID spectra of (a) ~3. 9ML NO_2/Au(111), (b) ~1.0 ML NO_2 on ^{16}O/Au(111), $\theta_o \approx 0.95$ ML; (c) 15 s NO on ^{18}O/Au(111), $\theta_o \approx 0.95$ ML, $m/z \sim 32$; (d) 15 s NO on ^{18}O/Au(111), $\theta_o \approx 0.95$ ML, $m/z \sim 30$. The Kr beam (~1 eV) strikes the sample at $t = 10$ s. Inset: TPD spectra before (e) and after (f) a typical Kr sweep experiment. NO beam flux (F): $\sim 1 \times 10^{13}$ molecules cm^{-2} s^{-1}.

the NO + O reaction on the Au(111) surface occurs at the periphery of oxidized regions of the O/Au(111) surface, where locally the surface may be more similar to clean Au(111). While we stress the very speculative nature of our argument, these results do illustrate the interesting chemistry NO_2 can exhibit on gold surfaces.

Collision Induced Desorption (CID) Measurements. While TPR spectra, such as those shown in Figure 6, suggest that NO_2 can be formed from NO and O atoms on the Au(111) surface, they do not provide much insight regarding the temperature at which the NO_2 product is formed on the surface, only to the extent that it must occur between the NO dosing temperature ($T_s \approx 85$ K) and the NO_2 product desorption temperature ($T_s \approx 225$ K). Collision induced desorption (CID) measurements were performed in an attempt to determine the temperature at which the coadsorbed NO and O atoms react on the Au(111) surface. Collision induced desorption (CID) measurements provide a method of probing adsorbed species on the Au(111) surface by using the QMS mass spectrometer *without* having to necessarily heat the sample to desorb and detect surface bound species. Thus, by performing CID or Kr "sweep" measurements on Au(111) samples dosed with NO_2, NO_2, and adsorbed oxygen atoms, and NO coadsorbed with oxygen atoms, we can hope to gain some information regarding the reaction products present at low temperatures ($T_s \approx 85$ K) on Au samples *unperturbed* by any heating.

Figure 7 shows the results of several CID measurements performed on Au(111) samples dosed with NO_2, NO_2 coadsorbed with O atoms, and NO coadsorbed with O^{18} atoms. As Figure 7 illustrates, no NO_2 is swept from the sample when NO_2 is chemisorbed to the clean (Figure 7a) or oxygen covered (Figure 7b) Au(111) surface, as evidenced by the absence of any $m/z \sim 30$ signal during the CID measurements. These results suggest that if coadsorbed NO and oxygen atoms produce a surface bound NO_2 product on the Au(111) surface at $T_s \approx 85$ K (with or without the presence of additional oxygen adatoms), *no* signal will be observed during the Kr "sweep". When NO is coadsorbed with isotopically labeled ^{18}O atoms at a temperature of $T_s \approx 85$ K and swept with the Kr beam, a small amount of $m/z \sim 30$ ($N^{16}O$) is shown to evolve from the sample surface (Figure 7d). During this same CID experiment, no $m/z \sim 32$ ($N^{18}O$) signal is observed to evolve from the surface (Figure 7c). The inset of Figure 7 shows TPD spectra obtained from surfaces co-dosed with ^{16}O atoms and NO at $T_s \approx 85$ K that *have* been swept prior to TPD heating (Figure 7f) and *have not* been swept prior to TPD heating (Figure 7e). Comparison of these TPD spectra shows that the low-temperature NO desorption peak present at $T_s \approx 105$ K in the unswept sample (Figure 7e) can be removed by an impinging Kr beam and thus is not present in the swept sample TPD spectra (Figure 7f). However, the NO_2 desorption feature at $T_s \approx 225$ K remains present in *both* the swept and unswept samples. It should be noted that the integrated peak area under the $T_s \approx 105$ K desorption feature in curve e is equivalent to the integrated area of NO removed during a Kr sweep experiment (curve d). When NO is coadsorbed with isotopically labeled ^{18}O adatoms (a preparation similar to that shown for curves c and d of Figure 7) the low-temperature NO desorption feature ($T_s \approx 105$ K) shows no isotopic mixing, i.e., there is no $m/z \sim 32$ signal coincident with this desorption feature. Isotopic mixing is observed in the NO_2 desorption feature at $T_s \approx 225$ K when NO is coadsorbed with ^{18}O atoms, similar to the mixing observed in Figure 6B.

It was also shown previously in Figure 1 that NO adsorbed to the clean, bulk gold surface (steps or defects) can be removed from the sample by CID. No TPD feature corresponding to NO adsorbed on the clean Au(111) surface ($T_s \approx 150$ K) was observed during the TPD heating of samples containing coadsorbed NO and O atoms.

From these CID results, we speculate that the NO species which desorbs from the oxygen covered Au(111) sample at $T_s \approx 105$ K is an adsorbed, unreacted NO molecule that resides on the O/Au(111) surface. This assertion is supported by (i) the lack of isotopic mixing of this feature when NO is coadsorbed with ^{18}O atoms on the Au(111) surface and (ii) the presence of a NO_2 desorption feature at $T_s \approx 225$ K (with the same integrated area) for both the swept (Figure 7f) and unswept (Figure 7e) samples. Assuming first-order desorption kinetics, and a desorption preexponential value of $\nu_d \approx 10^{13}$ s^{-1}, a Redhead desorption activation energy of approximately $E_d \approx 0.28$ eV is estimated for NO adsorbed on O/Au(111) ($\theta_o \approx 0.95$ ML).[37] It is also apparent from the CID measurements that not all of the NO that adsorbs to the oxygen covered Au(111) surface at $T_s \approx 85$ K can be completely removed by the Kr sweep, since equivalent NO_2 product desorption is seen for both the swept (Figure 7f) and unswept (Figure 7e) samples. These observations, coupled with the fact that (i) NO_2 cannot be swept from the clean or oxygen covered Au(111) at $T_s \approx 85$ K and (ii) NO can be swept from the clean or oxygen covered Au(111) at $T_s \approx 85$ K, *suggest* that NO can react to form a surface bound NO_2 product at temperatures as low as $T_s \approx 85$ K on the Au(111) surface. This hypothesis would be consistent with the CID/TPD measurements shown in Figure 7a−e.

Additional experiments were performed to estimate the percentage of NO adsorbed on the oxygen-covered Au(111) surface at $T_s \approx 85$ K that reacts to form NO_2 as a function of the initial oxygen adatom coverage, θ_o. These experiments were performed by *delivering* the same nitric oxide dose (15 s) to Au(111) samples of varying initial oxygen coverages. The surface was then heated and the relative areas underneath the unreacted NO desorption peak ($T_s \approx 105$ K) and the NO_2 desorption peak ($T_s \approx 225$ K) were compared. At lower oxygen coverages, ($\theta_o \approx 0.3$ ML), roughly ~75% of the adsorbed NO reacts to form the surface bound NO_2 product, with the remainder desorbing as unreacted, molecular NO at $T_s \approx 105$ K. At these lower oxygen coverages, most of the oxygen atoms

are consumed in the reaction (as determined during the subsequent recombinative O_2 TPD), which suggests that the relatively small amount of atomic oxygen initially present on the surface limits the complete conversion of the adsorbed nitric oxide. As the oxygen coverage is increased to $\theta_o \approx 0.95$ ML and above, the percentage of adsorbed NO that reacts to form NO_2 is roughly ~90%. This result suggests that although smaller amounts of NO adsorb on Au(111) samples with higher oxygen coverages (Figure 2), more oxygen adatoms are available for reaction with the adsorbed nitric oxide to form NO_2.

Reaction Activation Energy for NO + O(a) → NO_2 on Au(111). To obtain an estimate for the surface reaction activation energy, E_r, we employ the following simple kinetic model for the reaction of NO with atomic oxygen chemisorbed to the Au(111) surface. It should be noted that the structural nature of the oxygen species on the Au(111) surface is not well understood at present. It is well-documented in the literature that Au surfaces exposed to ozone,[14] oxygen plasma sources,[44] and DC ion sputtering[11,45] can produce a gold oxide (Au_xO_y) surface species, especially at higher atomic oxygen coverages ($\theta_o \approx 1$ ML and above).[41] Thus, the employed mechanism is a rather simple one. A full understanding of the chemical behavior of oxygen atoms on gold may be required to develop a complete picture of this NO oxidation reaction and other oxidation reactions occurring on bulk gold surfaces.

In our simple kinetic model, the NO molecule first enters a weakly bound state on the O/Au(111) surface from the gas phase, and from previous studies of adsorbate/surface trapping in the literature (CH_4/Ir(111),CH_4/Ir(110);[46] Ar/Pt(111);[47] N_2/W(100)[48]) we expect a temperature independent trapping coefficient over the relatively limited temperature range of our experiments ($T_s \approx 77-400$ K). Once the NO molecule is weakly bound to the Au surface a kinetic competition occurs between desorption of the NO molecule or adsorption/reaction with the coadsorbed O atoms. Once NO_2 is formed it can either remain on the surface or desorb. This reaction scheme is shown below in eqs 1−3.

$$NO(g) \underset{\alpha * Flux}{\overset{k_d}{\leftrightarrow}} NO(ads) \quad (1)$$

$$NO(ads) + O(ads) \xrightarrow{k_r} NO_2(ads) \quad (2)$$

$$NO_2(ads) \xrightarrow{k_{d2}} NO_2(g) \quad (3)$$

If we assume that at temperatures above the NO_2 desorption temperature ($T_s \approx 225$ K) (and subsequently above the NO desorption temperature), adsorbed NO either (a) reacts with coadsorbed atomic oxygen to promptly produce and desorb NO_2 or (b) desorbs back into the gas phase as NO, we may use spectra such as those in Figure 5 for $T_s > 225$ K to obtain *initial* NO_2 production rates for a given temperature and initial atomic oxygen coverage. Assuming temperature independent trapping for the NO molecule,[46−48] and the steady-state approximation for adsorbed NO ($d[NO(ads)]/dt \approx 0$) at these elevated temperatures, we may express the production of NO_2 as shown in eq 4, in which α is the temperature independent trapping

$$\frac{d[NO_2]}{dt} = k_r[NO(ads)][O(ads)] = \frac{\alpha F k_r[O(ads)]}{(k_d + k_r[O(ads)])} \quad (4)$$

coefficient and F is the constant NO molecular beam flux. At temperatures above $T_s \approx 200$ K, the k_d term in the denominator of (4) should be large compared to the $k_r[O(ads)]$ term found in the denominator. By using this simplifying approximation, eq 4 becomes

$$\frac{d[NO_2]}{dt} \approx k_r[NO(ads)][O(ads)] = \frac{\alpha F k_r[O(ads)]}{k_d} \quad (5)$$

and $N^{18}O$ production spectra for a given oxygen adatom coverage at temperatures above $T_s > 200$ K, such as those in Figure 5, and can be used to obtain relative initial NO_2 production rates. An Arrhenius plot of these initial $N^{18}O$ production rates can be constructed, eq 6, to estimate the activation energy for reaction of NO and O(ads).

$$\ln\left(\frac{d[NO_2]}{dt}\right) \approx \ln\left(\alpha F\left(\frac{\upsilon_r}{\upsilon_d}\right)[O(ads)]\right) + \frac{(E_d - E_r)}{k_b T} \quad (6)$$

An Arrhenius plot constructed for NO impinging on an Au(111) surface with $\theta_o \approx 0.95$ ML oxygen coverage produces a linear plot with an activation energy difference, $E_d - E_r$, of 0.07 ± 0.02 eV (98% confidence interval). Using the estimate of $E_d \approx 0.28$ eV for the desorption activation energy of NO on *oxygen-covered* Au(111) gives an estimate of $E_r \approx 0.21 \pm 0.02$ eV for the reaction of NO and oxygen atoms on Au(111), with $\theta_o \approx 0.95$ ML atomic oxygen coverage. This value of $E_r \approx 0.21$ eV is consistent with the notion of NO reacting with adsorbed oxygen at $T_s \approx 85$ K.

The estimated activation energy for NO oxidation on oxygen covered Au(111) appears to be higher than the activation energy for CO oxidation by atomic oxygen on Au(110)-(1 × 2)[17] and Au(111),[18] which show a negligible activation energy for CO oxidation ($E_a \approx 0.09 \pm 0.05$ eV).[17] In their high-temperature, chemiluminesence study of NO_2 formation on polycrystalline Au, Ardebili and co-workers[26] produce an Arrhenius plot of the initial chemiluminesence vs surface temperature for a polycrystalline Au surface pre-covered with atomic oxygen (unknown coverage value). This plot has a slope that corresponds to an effective activation energy of $E_{r,eff} \approx 0.70 \pm 0.05$ eV. While this value is higher than our estimated reaction activation energy, a direct, quantitative comparison is difficult, since the oxygen coverages used in their study are not known. In general we would expect experimentally determined reaction activation energy values to be different for different initial atomic oxygen coverages. Additional $N^{18}O^+$ production reaction measurements (not shown) carried out at $T_s \approx 200$ K for different oxygen coverages show a decrease in the initial reaction rate for coverages greater than $\theta_o \approx 0.95$ ML and an increase in the initial reaction rate for coverages lower than $\theta_o \approx 0.95$ ML. Regardless, our high-temperature ($T_s \approx 200$ K) reaction data agree qualitatively with those of Ardebili et al., i.e., at higher surface temperatures the initial NO_2 production rate is suppressed.

Conclusions

An investigation of the adsorption and reaction of NO with atomic oxygen covered Au(111) was conducted under UHV conditions. It was shown that NO uptake on the Au(111) surface is enhanced by the presence of oxygen adatoms, which we speculate is due to changes (electronic and/or structural) in the Au surface induced by the presence of adsorbed oxygen atoms. Dosing of the oxygen covered Au(111) surface with nitric oxide results in the removal of oxygen atoms from the surface upon heating, as revealed by O_2 TPD spectra. This is attributed to the production of NO_2 from the reaction of the impinging NO and oxygen atoms residing on the Au(111) surface. At temper-

atures above $T_s \approx 200$ K, the data suggest that NO_2 production becomes limited by the surface lifetime of the adsorbed NO species. At temperatures below $T_s \approx 200$ K, nitric oxide can react with surface oxygen to form a chemisorbed NO_2 product, observed in subsequent TPR spectra. A simple reaction mechanism for this system was proposed and was used to obtain an estimate for the activation energy for surface reaction ($E_r \approx 0.21 \pm 0.02$ eV) for NO with an O/Au(111) surface with $\theta_o \approx 0.95$ ML atomic oxygen coverage. CID and TPD spectra results suggest that NO may react with oxygen atoms on the surface at temperatures as low as $T_s \approx 85$ K. These results further illustrate that *atomic* oxygen covered bulk gold surfaces can be catalytically active.

Acknowledgment. The authors would like to thank the Welch Foundation (Grant F-1436) and the donors of the Petroleum Research Fund, administered by the American Chemical Society, for partial support of this study.

References and Notes

(1) Hammer, B.; Nørskov, J. K. *Nature* **1995**, *376*, 238−40.
(2) Bond, G. C.; Thompson, D. T. *Catal. Rev.* **1999**, *41*, 319.
(3) Haruta, M. *Catal. Today* **1997**, *36*, 153.
(4) Valden, M.; Lai, X.; Goodman, D. W. *Science* **1998**, *281*, 1647.
(5) Kim, T. S.; Stiehl, J. D.; Reeves, C. T.; Meyer, R. J.; Mullins, C. B. *J. Am. Chem. Soc.* **2003**, *125*, 2018.
(6) Daté, M.; Ichihashi, Y.; Yamashita, T.; Chiorino, A.; Bocucuzzi, F.; Haruta, M. *Catal. Today* **2002**, *72*, 89.
(7) Haruta, M. *CATTECH* **2002**, *6*, 102.
(8) Ueda, A.; Haruta, M. *Gold Bull.* (*Geneva*) **1999**, *32*, 3.
(9) Boccuzzi, F.; Chiorino, A. *J. Phys. Chem. B* **2000**, *104*, 5414.
(10) Bondzie, V. A.; Parker, S. C.; Campbell, C. T. *Catal. Lett.* **1999**, *63*, 143.
(11) Pireaux, J. J.; Chtaib, M.; Delrue, J. P.; Thiry, P. A.; Liehr, M.; Cuadano, R. *Surf. Sci.* **1984**, *141*, 221.
(12) Eley, D. D.; Moore, P. B. *Surf. Sci.* **1978**, *76*, L599.
(13) Sault, A. J.; Madix, R. J.; Cambpell, C. T. *Surf. Sci.* **1986**, *169*, 347.
(14) Saliba, N.; Parker, D. H.; Koel, B. E. *Surf. Sci.* **1998**, *410*, 270.
(15) Gottfried, J. M.; Schmidt, K. J.; Schroeder, S. L. M.; Christmann, K. *Surf. Sci.* **2002**, *511*, 65.
(16) Outka, D. A.; Madix, R. J. *J. Am. Chem. Soc.* **1987**, *109*, 1708.
(17) Outka, D. A.; Madix, R. J. *Surf. Sci.* **1987**, *179*, 361.
(18) Kim, T. S.; Stiehl, J. D.; McClure, S. M.; Tanaka, P. L.; Mullins, C. B. In preparation.
(19) Lagaza, M. A.; Wickham, D. T.; Parker, D. H.; Kastanas, G. N.; Koel, B. E. *Selective Catalytic Oxidation*; ACS Symp. Ser. 523; American Chemical Society: Washington, DC, 1993; p 90.
(20) Bollinger, M. J.; Sievers, R. E.; Fahey, D. W.; Fehsenfeld, F. C. *Anal. Chem.* **1983**, *55*, 1980.
(21) Toda, K.; Ochi, K.; Sanemasa, I. *Sens. Actuators B* **1996**, *32*, 15.
(22) Roh, S.; Stetter, J. R. *J. Electrochem. Soc.* **2003**, *150*, H272.
(23) Yu, A.; Liang, Z.; Cho, J.; Caruso, F. *Nano Lett.* **2003**, *3*, 1203.
(24) Bartram, M. E.; Koel, B. E. *Surf. Sci.* **1989**, *213*, 137.
(25) Wang, J.; Koel, B. *Surf. Sci.* **1999**, *436*, 15.
(26) Ardebili, M. H. P.; Grice, R.; Hodgson, M. E.; Hughes, C. J.; Whitehead, J. C. *J. Chem. Soc., Faraday Trans.* **1992**, *88* (10), 1377.
(27) Sato, S.; Senga, T.; Kawasaki, M. *J. Phys. Chem. B* **1999**, *103*, 5063. During their investigation of the photochemistry of NO_2 adsorbed on Au(111) these authors state that they observed nitric oxide reacting with atomic oxygen on Au(111) to form NO_2. However, no data are presented in this investigation, or to our knowledge have been presented since this publication.
(28) Wheeler, M. C.; Seets, D. C.; Mullins, C. B. *J. Chem. Phys.* **1996**, *105*, 1572.
(29) Stiehl, J. D.; Kim, T. S.; McClure, S. M.; Mullins, C. B. *J. Am. Chem. Soc.* **2004**, *126*, 1606. Stiehl, J. D.; Kim, T. S.; Reeves, C. T.; Meyer, R. J.; Mullins, C. B. *J. Phys. Chem. B* **2004**, *108*, 7917.
(30) Pollard, J. E. *Rev. Sci. Instrum.* **1992**, *63*, 1771.
(31) Wheeler, M. C.; Seets, D. C.; Mullins, C. B. *J. Chem. Phys.* **1997**, *107*, 1672.
(32) Wheeler, M. C.; Reeves, C. T.; Seets, D. C.; Mullins, C. B. *J. Chem. Phys.* **1998**, *108*, 3057.
(33) Gland, J. L. *Surf. Sci.* **1980**, *93*, 487.
(34) Canning, N. D. S.; Outka, D.; Madix, R. J. *Surf. Sci.* **1984**, *141*, 240.
(35) Beckerle, J. D.; Johnson, A. D.; Ceyer, S. T. *Phys. Rev. Lett.* **1989**, *62*, 685.
(36) King, D. A.; Wells, M. G. *Proc. R. Soc. London, Ser. A* **1974**, *339*, 245.
(37) Redhead, P. A. *Vacuum* **1962**, *12*, 203.
(38) Endou, A.; Ohashi, N.; Yoshizawa, K.; Takami, S.; Kubo, M.; Miyamoto, A.; Broclawik, E. *J. Phys. Chem. B* **2000**, *104*, 5110.
(39) Debeila, M. A.; Coville, N. J.; Scurrell, M. S.; Hearne, G. R. *Catal. Today* **2002**, *72*, 79.
(40) Solymosi, F.; Bánsági, T.; Zakar, T. S. *Catal. Lett.* **2003**, *87*, 7.
(41) Gottfried, J. M.; Schmidt, K. J.; Schroeder, S. L. M.; Christmann, K. *Surf. Sci.* **2003**, *525*, 197.
(42) Feibelman, P. J.; Hamann, D. R. *Phys. Rev. Lett.* **1983**, *52*, 61.
(43) Benndorf, C.; Madey, T. E. *Chem. Phys. Lett.* **1983**, *101*, 59.
(44) Tsai, H.; Hu, E.; Perng, K.; Chen, M.; Wu, J. C.; Chang, Y. S. *Surf. Sci. Lett.* **2003**, *537*, L447.
(45) Gottfried, J. M.; Elghobashi, N.; Schroeder, S. L. M.; Christmann, K. *Surf. Sci.* **2003**, *523*, 89.
(46) Sitz, G. O.; Mullins, C. B. *J. Phys. Chem. B* **2002**, *106*, 8349.
(47) Mullins, C. B.; Rettner, C. T.; Auerbach, D. J.; Weinberg, W. H. *Chem. Phys. Lett.* **1989**, *163*, 111.
(48) Rettner, C. T.; Schweizer, E. K.; Stein, H.; Auerbach, D. J. *Phys. Rev. Lett.* **1988**, *61*, 986.